Surface Properties of Ground-State Nuclear Matter*

JOHN C. REYNOLDS†
Applied Mathematics Division, Argonne National Laboratory, Argonne, Illinois
(Received 4 January 1963)

A general method is derived for extending the many-body formalism of Martin and Schwinger to macroscopic inhomogeneous systems. This method is applied to the Puff-Martin approximation for nuclear matter and used to compute the properties of a plane nuclear surface. An iterative self-consistency computation is used, and a generalized effective-mass approximation is imposed to simplify the wave equation. The particle interaction is taken to be a separable Yamaguchi potential with an S-state hard shell. The results show a smoothly varying density and self-energy, with a surface thickness of 2.33 F. A calculation of the surface energy term in the Weizsäcker semiempirical mass formula gives 18.79 MeV.

I. INTRODUCTION

In previous papers by Puff and the present author,[1,2] an approximation based upon the general formalism of Martin and Schwinger[3] was developed for computing the ground-state properties of nuclear matter. In this paper, we consider the extension of this approximation (which we refer to as the Puff-Martin approximation) to inhomogeneous systems in order to calculate the properties of a plane surface of nuclear matter.

By considering the effect of an infinitesimal external potential upon a saturated many-body system at zero pressure, it can be shown that the Green's function equations which were derived by Martin and Schwinger for a homogeneous system are also capable of describing a macroscopic inhomogeneous system which possesses a surface. To extend the formalism to such an inhomogeneous situation it is only necessary to replace the boundary condition of spatial homogeneity by conditions on the limits of various properties at large distances from the surface.

This approach may be applied to the Puff-Martin approximation. However, since the inhomogeneous system must have zero pressure in order to possess a stationary surface, and since (as shown in Sec. IV of reference 1) the definition of the pressure is ambiguous in the Puff-Martin approximation, it is important to use an expression for the pressure which directly insures a stationary solution. We show that this requirement is met by the so-called "local-transport" expression for the pressure.

The Puff-Martin equations are essentially a self-consistency relation between a nonlocal, energy-dependent effective potential or self-energy and a spectral function. In the inhomogeneous case, they may be treated by expanding the spectral function as a product of wave functions. A solution may then be obtained iteratively by alternately computing wave functions from the self-energy and then a better self-energy from the wave functions. To simplify the equation for the wave functions we use a generalized effective-mass approximation, in which the self-energy is approximated by a quadratic function of momentum which is fitted to the true self-energy by least squares.

We have used this approach to compute the properties of a plane nuclear surface for the simple interparticle potential described in reference 1. The results show a smoothly varying density and self-energy, with a surface thickness of 2.33 F and a surface energy of 18.79 MeV.

Section II will describe the general extension of the Martin-Schwinger formalism to inhomogeneous systems. In Secs. III and IV this extension is applied to the Puff-Martin approximation to obtain equations for the wave functions and the self-energy. Section V will give numerical results and a derivation of the surface-energy term in the Weizsäcker semiempirical mass formula. We assume that the reader is familiar with the contents of reference 1 and refer to equations in that paper by using the numeral "I."

II. EXTENSION OF THE GENERAL FORMALISM TO THE INHOMOGENEOUS CASE

Fundamentally, the Martin-Schwinger formalism is based upon the description of a many-body system by a set of n-particle Green's functions which are defined as expectation values of time-ordered products of field operators,

$$G_n(1\cdots n;1'\cdots n')\equiv(-i)^n\exp[i\mu\textstyle\sum_i(t_i-t_i')]\times\langle T[\psi(1)\cdots\psi(n)\psi^\dagger(n')\cdots\psi^\dagger(1')]\rangle,$$

where the expectation value is taken over a complete ensemble of states with temperature $1/i\tau$ and chemical potential μ,

$$\langle X\rangle^{i\tau,\mu}=\mathrm{tr}e^{-i\tau(H-\mu N)}X/\mathrm{tr}e^{-i\tau(H-\mu N)}. \quad (1)$$

This ensemble may be reduced to the ground state by

* Supported in part by the U. S. Atomic Energy Commission and the Office of Scientific Research of the U. S. Air Force. Portions of the machine computations were supported by the Massachusetts Institute of Technology Computation Center.

† A portion of this work is based on a Ph.D. thesis submitted to Harvard University, May 1961, by the author, who was then a National Science Foundation Predoctoral Fellow.

[1] J. C. Reynolds and R. D. Puff, previous paper, Phys. Rev. 130, 1877 (1963).

[2] R. D. Puff, Ann. Phys. (N. Y.) 13, 317 (1961).

[3] P. C. Martin and J. Schwinger, Phys. Rev. 115, 1342 (1959).

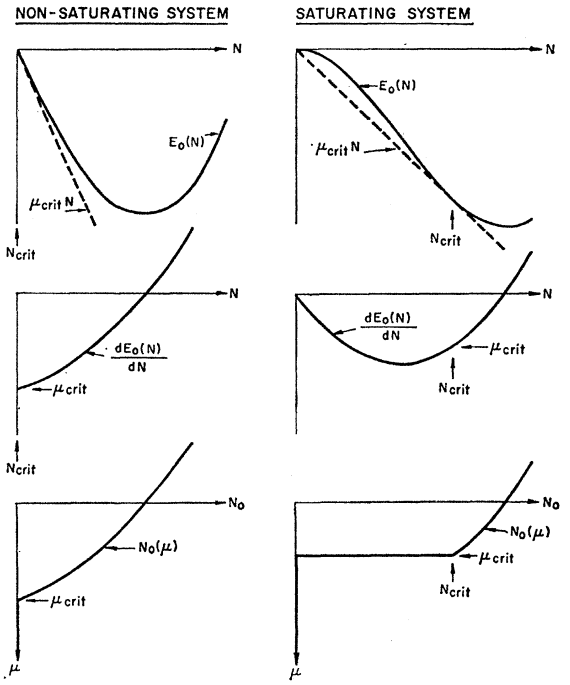

FIG. 1. General behavior of $E_0(N)$ and $N_0(\mu)$ for a nonsaturating and saturating system. These curves are only illustrative and do not represent quantitative results. In both cases the upper and middle curves represent $E_0(N)$ and dE_0/dN, respectively, while the lower curves (when viewed sideways) represent $N_0(\mu)$, which is the true minimum of $E_0(N)-\mu N$ for a given μ. The quantities N_{crit} and μ_{crit} are the grazing point and slope of the tangent to $E_0(N)$ which passes through the origin. When $\mu>\mu_{crit}$ the local minimum of $E_0(N)-\mu N$ is the true minimum, so that $N_0(\mu)$ is the inverse function of dE_0/dN. When $\mu<\mu_{crit}$, the true minimum of $E_0(N)-\mu N$ is $N_0(\mu)=0$. For the saturating system $N_{crit}>0$, and $N_0(\mu)$ jumps discontinuously from N_{crit} to zero at $\mu=\mu_{crit}$.

taking the low-temperature limit:

$$\lim_{i\tau\to\infty}\langle X\rangle^{i\tau,\mu}=\langle N,E_0(N)|X|N,E_0(N)\rangle|_{N=N_0(\mu)}, \quad (2)$$

where $E_0(N)$ is the ground-state energy of N particles and $N_0(\mu)$ is the value of N such that $E_0(N)-\mu N$ is a minimum.

Before considering the extension of this formalism to an inhomogeneous system, it is necessary to establish certain properties of $N_0(\mu)$. For a macroscopic system N may be considered as a continuous variable, and it is usually asserted that the minimum $N_0(\mu)$ is determined by

$$\frac{d}{dN}[E_0(N)-\mu N]\Big|_{N=N_0(\mu)}=\frac{dE_0}{dN}-\mu\Big|_{N=N_0(\mu)}=0, \quad (3)$$

with the additional condition

$$\frac{d^2}{dN^2}[E_0(N)-\mu N]\Big|_{N=N_0(\mu)}=\frac{d^2E_0}{dN^2}\Big|_{N=N_0(\mu)}>0. \quad (4)$$

However, this is actually an oversimplification; the function $E_0(N)-\mu N$ may have one or more local minima which satisfy Eqs. (3) and (4), and the values of the function at these points may or may not be less than the value $E_0(N)-\mu N=0$ at the end point $N=0$. Furthermore, the true minimum $N_0(\mu)$ may jump discontinuously from one local minimum to another or to the end point as μ is varied.

We limit ourselves to the case of a single local minimum. For large μ, the true minimum $N_0(\mu)$ will be the local minimum and will satisfy Eqs. (3) and (4), but for sufficiently negative μ the true minimum will be the end point $N_0(\mu)=0$. Let N_{crit}, μ_{crit} be the point at which the local minimum ceases to be the true minimum. This point will satisfy Eq. (3) and the additional condition that $E_0(N)-\mu N$ have the same value at N_{crit}, μ_{crit} as at $N=0$,

$$E_0(N)-\mu N|_{N_{crit},\mu_{crit}}=E_0(N)-\mu N|_{N=0}=0. \quad (5)$$

Thus, this point is determined by

$$\mu_{crit}=\frac{dE_0}{dN}\Big|_{N=N_{crit}}=\frac{E_0(N)}{N}\Big|_{N=N_{crit}}, \quad (6)$$

and $N_0(\mu)$ will be discontinuous at this point if $N_{crit}>0$. It is shown in reference 1 that Eq. (6) implies (for an exact solution) that N_{crit}, μ_{crit} is the point (called the zero point) at which the pressure of the system is zero. Thus, the existence of a discontinuity in $N_0(\mu)$ is associated with the physical characteristic of saturation, since $N_{crit}>0$ implies the existence of an unrestrained or zero-pressure system of particles with finite density. Figure 1 exhibits the general relation between $E_0(N)$ and $N_0(\mu)$ for a nonsaturating and saturating system.

We may expect that an actual solution of the usual Green's function equations for a saturating system will not explicitly exhibit a discontinuity at the zero point, but rather that the equations will possess two distinct solutions (within some region of μ containing μ_{crit}): an ordinary finite-density solution for which $\mu=dE_0/dN$, and an extraordinary solution describing a vacuum. The discontinuity must then be imposed by switching from the ordinary to the vacuum solution at $\mu=\mu_{crit}$. (It should be noted that the vacuum solution for G_1, since it describes a single particle propagating through the vacuum, is independent of the interparticle potential and, therefore, equal to the analogous function for free particles.) In dealing with a homogeneous system (as in reference 1) it is justifiable to ignore the extraordinary solution and consider the ordinary solution for $\mu<\mu_{crit}$ as a description of a metastable system with negative pressure. However, an explicit consideration of the zero-point discontinuity is necessary to justify the extension of the Green's function formalism to inhomogeneous systems.

To develop this extension we note that the definition of the Green's functions implies that a translationally invariant Hamiltonian will lead to Green's functions

which are spatially homogeneous, i.e., which depend only upon the difference of their spatial variables, and must, therefore, describe a homogeneous system. This suggests that inhomogeneous systems may be approached by introducing an infinitesimal external potential which will appear in the Hamiltonian as an additional term,

$$H_{\text{ext}}=\int d\mathbf{r}\, V_{\text{ext}}(\mathbf{r})\psi^{\dagger}(\mathbf{r}t)\psi(\mathbf{r}t). \tag{7}$$

The introduction of this potential modifies the integro-differential equations (I.1) for the G_n by replacing the differential operator

$$\left[i\frac{\partial}{\partial t_1}+\frac{\nabla_1^2}{2m}+\mu\right] \text{ by } \left[i\frac{\partial}{\partial t_1}+\frac{\nabla_1^2}{2m}+\mu-V_{\text{ext}}(\mathbf{r}_1)\right]. \tag{8}$$

In particular, we consider a saturated system at zero pressure ($\mu=\mu_{\text{crit}}$) which is subjected to an external potential with the form of an infinitesimal well

$$\begin{aligned} V_{\text{ext}}(\mathbf{r})&=-\epsilon, \ \mathbf{r} \text{ in } R_0 \\ &=\epsilon, \ \mathbf{r} \text{ not in } R_0; \quad \epsilon>0, \end{aligned} \tag{9}$$

in the macroscopic region R_0. Physically we expect that a bound aggregate of particles will be localized in the well since there will be no back pressure against the well and since a macroscopic well will have a vanishing zero-point energy. On the other hand, the infinitesimal well edge should not have any distorting effect on the surface of the aggregate. Thus the Green's functions near the surface of R_0 should describe a localized but undistorted surface of saturated matter.

Mathematically, since V_{ext} is subtracted from μ in the Green's function equations, the local properties of the system at large distances from the surface of R_0 should approach the properties of a homogeneous system for $\mu=\mu_{\text{crit}}+\epsilon$ inside the well, and for $\mu=\mu_{\text{crit}}-\epsilon$ outside the well. Thus, since the homogeneous system jumps discontinuously from a finite density at $\mu_{\text{crit}}+\epsilon$ to a vacuum at $\mu_{\text{crit}}-\epsilon$, we see that the expected physical situation is realized.

Now we have suggested that the discontinuity of μ_{crit} is not inherent in the equations for the homogeneous Green's functions but must be imposed by switching from an ordinary solution to the vacuum solution. In this situation, the infinitesimal external potential may be neglected in the inhomogeneous-case equations, so that the inhomogeneous functions will satisfy the same equations as in the homogeneous case. The only change is that the implied boundary condition of spatial homogeneity must be replaced by conditions which specify that the local properties of the system approach the properties of saturated homogeneous matter inside R_0 and approach the properties of the vacuum outside R_0. These local properties include the Green's functions themselves, which are local properties of their average spatial coordinate.

The simplest possible inhomogeneous geometry is that of a single plane surface of matter localized by choosing R_0 to be the half-space $Z>0$. In this case, the local properties of the system are spatially inhomogeneous only along the z axis, approaching the properties of homogeneous matter as $Z\rightarrow+\infty$, and of the vacuum as $Z\rightarrow-\infty$. In the following sections we obtain solutions for nuclear matter in this geometry, using the Puff-Martin approximation.

III. APPLICATIONS TO NUCLEAR MATTER; THE WAVE FUNCTIONS

In reference 1, the approximate Puff-Martin equations for G_1 and G_2 were derived and manipulated (without using the condition of spatial homogeneity) into Eqs. (I.39),

$$\Sigma(\mathbf{r}_1\mathbf{r}_1'\omega)=\int_{-\infty}^{0}\frac{d\omega'}{2\pi}\int d\mathbf{r}_2 d\mathbf{r}_2'\int\frac{d\mathbf{K}}{(2\pi)^3}\exp\left[i\mathbf{K}\cdot\left(\frac{\mathbf{r}_1+\mathbf{r}_2}{2}-\frac{\mathbf{r}_1'+\mathbf{r}_2'}{2}\right)\right]\langle\mathbf{r}_1-\mathbf{r}_2|\,T_{\mathbf{K}}(\omega+\omega')\,|\mathbf{r}_1'-\mathbf{r}_2'\rangle A(\mathbf{r}_2'\mathbf{r}_2\omega'), \tag{10}$$

and (I.40),

$$[\omega+\nabla^2/2m+\mu]G(\mathbf{r}\mathbf{r}'\omega)-\int d\mathbf{r}''\,\Sigma(\mathbf{r}\mathbf{r}''\omega)G(\mathbf{r}''\mathbf{r}'\omega)=\delta(\mathbf{r}-\mathbf{r}'), \tag{11}$$

which determine a self-energy function $\Sigma(\omega)$ and a spectral function $A(\omega)$ which is the discontinuity of $G(\omega)$ across the real ω axis,

$$A(\mathbf{r}\mathbf{r}'\omega)=\lim_{\epsilon\rightarrow+0}\frac{1}{i}[G(\mathbf{r}\mathbf{r}'\omega-i\epsilon)-G(\mathbf{r}\mathbf{r}'\omega+i\epsilon)]. \tag{12}$$

The function T is equivalent, except for the addition of $2\mu-\mathbf{K}^2/4m$ to the energy, to a sum of spin-isospin matrix elements of the scattering matrix for two particles in a vacuum. It should be noted that since T is independent of many-body effects it will be the same for homogeneous and inhomogeneous systems. According to Eqs. (I.8) and (I.9) (in the low-temperature limit) the number of particles and energy of the system may be expressed as volume integrals of a particle density

$$\rho(\mathbf{r})=\int_{-\infty}^{0}\frac{d\omega}{2\pi}A(\mathbf{r}\mathbf{r}\omega), \tag{13}$$

and an energy density

$$\epsilon(\mathbf{r})=\int_{-\infty}^{0}\frac{d\omega}{2\pi}\lim_{\mathbf{r}'\rightarrow\mathbf{r}}\frac{1}{2}\left[\omega-\frac{\nabla^2}{2m}+\mu\right]A(\mathbf{r}\mathbf{r}'\omega), \tag{14}$$

(which both must be multiplied by a degeneracy factor of 4).

To obtain solutions for a plane nuclear surface we must impose the boundary condition that $\Sigma(\mathbf{r}\mathbf{r}'\omega)$ and $A(\mathbf{r}\mathbf{r}'\omega)$ approach the corresponding functions for a vacuum and for homogeneous matter at zero pressure as $\frac{1}{2}(z+z')$ goes to $-\infty$ and $+\infty$, respectively. However, as is shown in Sec. IV of reference 1, several expressions for the pressure are available which lead to different results in the approximation, and therefore to different values of the homogeneous A and Σ at zero pressure. In computing the homogeneous solution which will be used in the boundary conditions for the inhomogeneous calculation, it is vital to use the particular pressure expression which will insure the existence of an inhomogeneous solution, or more precisely the existence of a time-independent solution such that

$$[\partial/\partial t+\partial/\partial t']G_1(\mathbf{r}t;\mathbf{r}'t')=0. \tag{15}$$

On the one hand, the requirement that the boundary condition solution have zero pressure is equivalent to requiring that the pressure of the inhomogeneous system be the same on both sides of the surface. On the other hand, Eq. (15) implies that the local momentum density

$$\mathcal{G}(\mathbf{r}t)=-\tfrac{1}{2}\lim_{\mathbf{r}'\to\mathbf{r}}(\nabla-\nabla')G_1(\mathbf{r}t;\mathbf{r}'t^+) \tag{16}$$

must be independent of time. Thus, the pressure relation must be chosen so that the spatial conservation of pressure will imply that the local momentum density is time-independent, when this density is computed from the approximate G_1. This requirement is satisfied by the local-transport expression for the pressure, which was derived in reference 1; therefore, the homogeneous A and Σ used as boundary conditions must be taken at the local-transport zero point.[4]

As in the homogeneous case, the self-consistent solution of Eqs. (10) and (11) as well as the computation of Eqs. (13) and (14) requires a knowledge of A only in the region $\omega<0$ for which Σ is continuous across the real ω axis. This continuity implies that for $\omega<0$ the spectral function A satisfies

$$[\omega+\nabla^2/2m+\mu]A(\mathbf{r}\mathbf{r}'\omega)-\int d\mathbf{r}''\,\Sigma(\mathbf{r}\mathbf{r}''\omega)A(\mathbf{r}''\mathbf{r}'\omega)=0,\quad \omega<0, \tag{17}$$

which is obtained by taking the discontinuity of Eq. (11) across the real axis. The boundary conditions connecting $A(\mathbf{r}\mathbf{r}'\omega)$ to the homogeneous A are sufficient to establish the correct normalization.

Since A and Σ are spatially inhomogeneous only along the z axis, it is convenient to subject them to a partial Fourier transformation in which their spatial difference variables along the x and y axes are transformed into momentum space,

$$\Sigma(\mathbf{r}\mathbf{r}'\omega)=\int\frac{dk_xdk_y}{(2\pi)^2}\exp[ik_x(x-x')+ik_y(y-y')]\Sigma(zz'k_r\omega), \tag{18}$$

(and similarly for A), where $k_r=(k_x^2+k_y^2)^{1/2}$. This is related to the full-momentum transform of all three difference variables by

$$\Sigma(zz'k_r\omega)=\int\frac{dk_z}{2\pi}\exp[ik_z(z-z')]\Sigma\left(\frac{z+z'}{2},\mathbf{k},\omega\right). \tag{19}$$

The partial transformation of Eq. (17) gives

$$\left[\omega-\frac{k_r^2}{2m}+\frac{1}{2m}\frac{\partial^2}{\partial z^2}+\mu\right]A(zz'k_r\omega)-\int dz''\,\Sigma(zz''k_r\omega)A(z''z'k_r\omega)=0, \tag{20}$$

which implies that A may be expanded as a product of one-dimensional wave functions ψ which satisfy the wave equation

$$\left[\omega-\frac{k_r^2}{2m}+\frac{1}{2m}\frac{\partial^2}{\partial z^2}+\mu\right]\psi(zk_r\omega)-\int dz''\,\Sigma(zz''k_r\omega)\psi(z''k_r\omega)=0. \tag{21}$$

Now our boundary conditions on Σ specify that

$$\begin{aligned}\Sigma(zz'k_r\omega)&\to 0 && \text{as } \frac{z+z'}{2}\to-\infty,\\ &\to\int\frac{dk_z}{2\pi}\exp[ik_z(z-z')]\Sigma_{\text{hom}}(\mathbf{k}\omega) && \text{as } \frac{z+z'}{2}\to+\infty,\end{aligned} \tag{22}$$

where $\Sigma_{\text{hom}}(\mathbf{k}\omega)$ is the momentum-space effective potential for the homogeneous case. These conditions imply

[4] This fact was learned through painful experience. Originally the entire computation described in this paper was carried out for the μ zero point. The final iterative computation did not converge but instead led to a situation in which each result for the self-energy reproduced the result of the previous iteration displaced along the z axis (towards the vacuums ide) by about $\frac{1}{3}$ F. Further calculations suggested that a time-independent solution did not exist. Only at this point was the distinction between the various zero points realized and the local-transport zero point derived and shown to be appropriate.

that as $z\to+\infty$ the wave functions will become one-dimensional plane waves with a wave number k_{z0} which satisfies

$$\omega=\omega_0((k_r^2+k_{z0}^2)^{1/2}), \tag{23}$$

where

$$\omega_0(\mathbf{k})=\frac{\mathbf{k}^2}{2m}+\Sigma_{\rm hom}(\mathbf{k},\omega_0(\mathbf{k}))-\mu. \tag{24}$$

The conditions also specify the multiplicity of the wave functions for various ω, and thereby determine the explicit expansion of A to be

$$\begin{aligned} A(zz'k_r\omega)&=0, && \omega<\omega_0(k_r);\\ &=\psi(zk_r\omega)\psi^*(z'k_r\omega), && \omega_0(k_r)<\omega<k_r^2/2m-\mu;\\ &=\psi_1(zk_r\omega)\psi_1^*(z'k_r\omega)+\psi_2\psi_2^*, && k_r^2/2m-\mu<\omega. \end{aligned} \tag{25}$$

Since $\mu<0$, our restriction to $\omega<0$ eliminates the third possibility, and restricts k_r to be smaller than the quantity k_f which satisfies $\omega_0(k_f)=0$. Essentially we are dealing with wave functions which are nondegenerate and semibound.

As $z\to+\infty$ the wave functions will approach a limit of the form

$$\psi(zk_r\omega)\underset{z\to+\infty}{\longrightarrow} c\sin[k_{z0}z+\eta(k_{z0})], \tag{26}$$

so that

$$A(zz'k_r\omega)\underset{z,z'\to+\infty}{\longrightarrow}\frac{|c|^2}{2}\{\cos[k_{z0}(z-z')]-\cos[k_{z0}(z+z')+2\eta(k_{z0})]\}. \tag{27}$$

The normalization constant c may be determined by comparing the first term of Eq. (27) with the homogeneous A, since the second term will become rapidly oscillating for large z and z' and will vanish in any integration over k_{z0}. The homogeneous A is given in momentum space by Eqs. (I.44) and (I.45) as

$$A_{\rm hom}(\mathbf{k}\omega)=2\pi\rho(\mathbf{k})\delta[\omega-\omega_0(\mathbf{k})], \tag{28}$$

where

$$\rho(\mathbf{k})=\left[1-\frac{\partial}{\partial\omega}\Sigma_{\rm hom}[\mathbf{k},\omega_0(\mathbf{k})]\right]^{-1}. \tag{29}$$

Thus, the partially transformed $A_{\rm hom}$ is

$$\begin{aligned} A_{\rm hom}(zz'k_r\omega)&=\frac{2k_0\rho(k_0)\cos k_{z0}(z-z')}{k_{z0}d\omega_0(k_0)/dk}\\ &=\left[\frac{k_{z0}}{2m}+\frac{k_{z0}}{2k_0}\frac{\partial}{\partial k}\Sigma_{\rm hom}[k_0,\omega_0(k_0)]\right]^{-1}\\ &\quad\times\cos k_{z0}(z-z'), \end{aligned} \tag{30}$$

where $k_0=(k_{z0}^2+k_r^2)^{1/2}$. This establishes the normalization constant as

$$c=\left[\frac{k_{z0}}{4m}+\frac{k_{z0}}{4k_0}\frac{\partial}{\partial k}\Sigma_{\rm hom}(k_0,\omega_0(k_0))\right]^{-1/2}, \tag{31}$$

where the phase has been chosen to yield real wave functions.

Now even for numerical calculation the wave equation (21) will be reasonably tractable only if the self-energy has a simple momentum dependence. Therefore, in our calculation we have used a generalized effective-mass approximation in which the full-momentum transform of Σ in its difference variables is restricted to being even and quadratic. However, Σ cannot be assumed *a priori* to be independent of the angle between its momentum argument and the z axis, so that the approximation

$$\tilde{\Sigma}(Z\mathbf{k}\omega)=\Sigma_0(Z\omega)+\Sigma_\perp(Z\omega)k_r^2+\Sigma_{\rm II}(Z\omega)k_z^2 \tag{32}$$

must be used. Substitution of this form into Eqs. (19) and (21) gives a generalized Schrödinger equation,

$$\frac{\partial}{\partial z}\left[\left(\Sigma_{\rm II}(z\omega)+\frac{1}{2m}\right)\frac{\partial}{\partial z}\psi(zk_r\omega)\right]=\left[-\omega+\frac{k_r^2}{2m}-\mu+\Sigma_0(z\omega)+\Sigma_\perp(z\omega)k_r^2-\frac{1}{4}\frac{\partial^2}{\partial z^2}\Sigma_{\rm II}(z\omega)\right]\psi(zk_r\omega), \tag{33}$$

which may be reduced by the substitution

$$\psi(zk_r\omega)=\left[\Sigma_{\rm II}(z\omega)+\frac{1}{2m}\right]^{-1/2}\phi(zk_r\omega) \tag{34}$$

to

$$\frac{\partial^2}{\partial z^2}\phi(zk_r\omega)=\left\{\frac{-\omega+k_r^2/2m-\mu+\Sigma_0(z\omega)+\Sigma_\perp(z\omega)k_r^2}{\Sigma_{\rm II}(z\omega)+1/2m}+\frac{1}{4}\frac{\partial}{\partial z}\left(\frac{\partial\Sigma_{\rm II}(z\omega)/\partial z}{\Sigma_{\rm II}(z\omega)+1/2m}\right)\right\}\phi(zk_r\omega). \tag{35}$$

To be consistent, we must also use the effective-mass approximation in calculating the homogeneous functions

used as boundary conditions. Thus, Σ_{hom} is approximated by a function of the form

$$\tilde{\Sigma}_{\text{hom}}(\mathbf{k}\omega)=\Sigma_{0\text{ hom}}(\omega)+\Sigma_{2\text{ hom}}(\omega)\mathbf{k}^2, \tag{36}$$

where there is no longer any dependence on the direction of $\mathbf{k}$. The substitution of this approximate form into Eq. (31) reduces the normalization constant to

$$c=\left[\frac{k_{z0}}{4m}+\frac{k_{z0}}{2}\Sigma_{2\text{ hom}}[\omega_0(k_0)]\right]^{-1/2}. \tag{37}$$

IV. THE SELF-ENERGY

We must now express the self-energy in terms of the wave-function expansion of A. By transforming Eq. (10) into an equation for the full-momentum transform of Σ in terms of the partial transform of A, and using the wave-function expansion (25), we obtain

$$\Sigma(Z_1\mathbf{k}_1\omega)=\int d\mathbf{R}_2\int\frac{d\mathbf{k}_2}{(2\pi)^3}\int_{-\infty}^{0}\frac{d\omega'}{2\pi}\left\{\int d\mathbf{r}\exp[-\tfrac{1}{2}i(\mathbf{k}_1-\mathbf{k}_2)\cdot\mathbf{r}]\langle\mathbf{R}_1-\mathbf{R}_2+\tfrac{1}{2}\mathbf{r}|\,T_{\mathbf{k}_1+\mathbf{k}_2}(\omega+\omega')\,|\,\mathbf{R}_1-\mathbf{R}_2-\tfrac{1}{2}\mathbf{r}\rangle\right\}$$
$$\times\int dz_2\exp[-ik_{z2}z_2]\psi(Z_2+\tfrac{1}{2}z_2,\,k_{r2},\,\omega')\psi^*(Z_2-\tfrac{1}{2}z_2,\,k_{r2},\,\omega'). \tag{38}$$

To use the effective-mass approximation we must approximate this function by the quadratic form (32). To minimize the error of this approximation we use a least-squares technique, choosing the functions Σ_0, $\Sigma_\perp$, and $\Sigma_{\|}$ to minimize a weighted integral of the difference between the approximate and exact Σ's,

$$\xi(Z\omega)=\int d\mathbf{k}\,W(\mathbf{k})[\Sigma_0(Z\omega)+\Sigma_\perp(Z\omega)k_r^2+\Sigma_{\|}(Z\omega)k_z^2-\Sigma(Z\mathbf{k}\omega)]^2. \tag{39}$$

Since the exact Σ will not exhibit a quadratic behavior for large $\mathbf{k}$, the weight function W must go to zero rapidly as $k\longrightarrow\infty$. A reasonable and simple choice is

$$W(\mathbf{k})=\exp[-\mathbf{k}^2/\beta^2], \tag{40}$$

where the constant β will be left arbitrary. By setting the derivatives of ξ with respect to Σ_0, $\Sigma_\perp$, and $\Sigma_{\|}$ equal to zero, we obtain

$$\Sigma_i(Z\omega)=\textstyle\sum_j M_{ij}U_j(Z\omega), \tag{41}$$

where M is the matrix

	0	$\perp$	$\|$
0	$\frac{5}{2}$	$-\beta^{-2}$	$-\beta^{-2}$
$\perp$	$-\beta^{-2}$	β^{-4}	0
$\|$	$-\beta^{-2}$	0	$2\beta^{-4}$

(42)

and

$$U_j(Z_1\omega)=\frac{1}{\beta^3\pi^{3/2}}\int d\mathbf{k}\,e^{-\mathbf{k}^2/\beta^2}\Sigma(Z_1\mathbf{k}\omega)\times\begin{Bmatrix}1, & j=0\\ k_r^2, & j=\perp\\ k_z^2, & j=\|\end{Bmatrix}=\int d\mathbf{R}_2dz_2\int_{k_{r2}<k_f}\frac{dk_{x2}dk_{y2}}{(2\pi)^2}\int_{\omega_0(k_{r2})}^{0}\frac{d\omega'}{2\pi}\frac{1}{\beta^3\pi^{3/2}}$$
$$\times\int d\mathbf{k}_1\,e^{-\mathbf{k}_1^2/\beta^2}\times\begin{Bmatrix}1, & j=0\\ k_{r1}^2, & j=\perp\\ k_{z1}^2, & j=\|\end{Bmatrix}\times\int\frac{dk_{z2}}{2\pi}e^{-ik_{z2}z_2}\int d\mathbf{r}\exp[-\tfrac{1}{2}i(\mathbf{k}_1-\mathbf{k}_2)\cdot\mathbf{r}]$$
$$\times\langle\mathbf{R}_1-\mathbf{R}_2+\tfrac{1}{2}\mathbf{r}|\,T_{\mathbf{k}_1+\mathbf{k}_2}(\omega+\omega')\,|\,\mathbf{R}_1-\mathbf{R}_2-\tfrac{1}{2}\mathbf{r}\rangle\psi(Z_2+\tfrac{1}{2}z_2,\,k_{r2},\,\omega')\psi^*(Z_2-\tfrac{1}{2}z_2,\,k_{r2},\,\omega'), \tag{43}$$

and where we have inserted integration limits which exclude the region where $A=0$.

Unfortunately, the use of Eq. (43) to compute the self-energy from a table of wave functions would require a prohibitive amount of time even on a high-speed computer. To overcome this difficulty we use the artifice of approximating the scattering matrix T by a sum of terms with exponential energy dependence. This leads to a simplification of Eq. (43) which reduces the computation time by an order of magnitude. For the simple inter-

particle potential used in reference 1, the T matrix may be written as a sum of terms in which the spatial and energy dependencies are separated,

$$T_{\mathbf{K}}(\omega)=\frac{3}{4m\pi}[\theta_{yys}(\omega')\tau_{yys}+\theta_{yyt}(\omega')\tau_{yyt}+\theta_{ycs}(\omega')\tau_{ycs}+\theta_{yct}(\omega')\tau_{yct}+\theta_{cc}(\omega')\tau_{cc}]|_{\omega'=\omega+2\mu-\mathbf{K}^2/4m}, \tag{44}$$

where

$$\langle\mathbf{r}|\tau|\mathbf{r}'\rangle=\frac{1}{rr'}\times\begin{cases}e^{-\alpha r}e^{-\alpha r'}, & (yy)\\ e^{-\alpha r}\delta(r'-r_c)+e^{-\alpha r'}\delta(r-r_c), & (yc)\\ \delta(r-r_c)\delta(r'-r_c), & (cc)\end{cases}$$

and

$$\theta(\omega)=\left\{\frac{1}{\gamma}\left[1-\frac{\pi^2\lambda}{\alpha(\alpha+\gamma)^2}\right][1-e^{-2\gamma r_c}]+\frac{4\pi^2\lambda}{(\alpha^2-\gamma^2)^2}[e^{-\gamma r_c}-e^{-\alpha r_c}]^2\right\}^{-1}\times\begin{cases}-\dfrac{\pi^2\lambda}{\gamma}[1-e^{-2\gamma r_c}], & (yy)\\ \dfrac{2\pi^2\lambda}{\alpha^2-\gamma^2}[e^{-\gamma r_c}-e^{-\alpha r_c}], & (yc)\\ \left[1-\dfrac{\pi^2\lambda}{\alpha(\alpha+\gamma)^2}\right], & (cc).\end{cases}$$

Here, $\gamma=(-m\omega)^{1/2}$ and the combination $\theta_{cc}=(\theta_{ccs}+\theta_{cct})$ is introduced since $\tau_{ccs}=\tau_{cct}$.

In this expression we approximate the θ functions by

$$\theta_k(\omega)=\textstyle\sum_{L=1}^{7} C_{kL}\exp[\alpha_L\omega]. \tag{45}$$

Table I gives the coefficients of this approximation, which were obtained by choosing the α_L arbitrarily and determining the C_{kL} by least-squares matching over the region -500 MeV$<\omega<-30$ MeV. For the yy and yc functions the approximation has a maximum relative error in this region of less than 0.08%. Since θ_{cc} has a zero in this region its relative error is infinite, but its maximum absolute error is less than 1.0% of its value at -500 MeV and less than 0.1% of its value at -30 MeV.

By substituting Eqs. (44) and (45) into Eqs. (41) to (43), the three components of the self-energy may be expressed as

$$\Sigma_i(Z_1\omega)=\sum_{L=1}^{7}\exp[\alpha_L(\omega+\mu)]\int_0^{k_f}\frac{k_{r2}dk_{r2}}{2\pi}\int dZ_2dz_2\,K_{Li}(Z_2z_2k_{r2})$$
$$\times\int_{\omega_0(k_{r2})}^{0}\frac{d\omega'}{2\pi}\exp[\alpha_L(\omega'+\mu)]\psi(Z_1+Z_2+\tfrac{1}{2}z_2,\,k_{r2},\,\omega')\psi^*(Z_1+Z_2-\tfrac{1}{2}z_2,\,k_{r2},\,\omega'), \tag{46}$$

where the kernel K is given by

$$K_{Li}(Zz_2k_{r2})=\frac{3}{4m\beta^3\pi^{5/2}}\int dXdY\int d\mathbf{k}_1\,e^{-\mathbf{k}_1^2/\beta^2}\times\begin{cases}5/2-k_{r1}^2/\beta^2-k_{z1}^2/\beta^2, & i=0\\ -1/\beta^2+k_{r1}^2/\beta^4, & i=\perp\\ -1/\beta^2+2k_{z1}^2/\beta^4, & i=\parallel\end{cases}$$
$$\times\int\frac{dk_{z2}}{2\pi}e^{-ik_{z2}z_2}\int d\mathbf{r}\,e^{-\frac{1}{2}i(\mathbf{k}_1-\mathbf{k}_2)\cdot\mathbf{r}}\sum_k C_{kL}\exp\left[-\frac{\alpha_L}{4m}(\mathbf{k}_1+\mathbf{k}_2)^2\right]\langle\mathbf{R}+\tfrac{1}{2}\mathbf{r}|\,\tau_k\,|\,\mathbf{R}-\tfrac{1}{2}\mathbf{r}\rangle. \tag{47}$$

TABLE I. Parameters of exponential approximation for the scattering matrix.[a]

L	α_L (MeV^{-1})	C_{yys} (F^{-3})	C_{yyt} (F^{-3})	C_{ycs} (F^{-2})	C_{yct} (F^{-2})	C_{cc} (F^{-1})
1	0	−45.911	−139.633	6.7168	16.8971	6.6573
2	1/320	−22.324	−136.417	11.3835	38.067	−24.531
3	1/160	5.2630	18.7878	−4.1329	−7.6052	13.1313
4	1/80	−19.0556	−114.409	8.1311	29.783	−16.0706
5	1/40	−12.6734	−126.036	3.6526	28.581	−4.4934
6	1/20	−25.249	−215.04	9.1383	52.000	−18.2438
7	1/10	−32.711	−550.95	10.4509	128.249	−30.512

[a] See Eqs. (44) and (45).

As we have noted, the effective-mass approximation must be applied not only to the inhomogeneous-case equations but also to the homogeneous-case equations which are solved to obtain the spatial boundary conditions. The homogeneous-case equations derived in reference 1 may be written as

$$\Sigma_{\rm hom}(\mathbf{k}_1,\omega)=\int_{|\mathbf{k}_2|<k_f} d\mathbf{k}_2\,\rho(\mathbf{k}_2)\left\langle\frac{\mathbf{k}_1-\mathbf{k}_2}{2}\left|T_{\mathbf{k}_1+\mathbf{k}_2}(\omega+\omega_0(\mathbf{k}_2))\right|\frac{\mathbf{k}_1-\mathbf{k}_2}{2}\right\rangle, \tag{48}$$

where

$$\rho(\mathbf{k}_2)=\left[1-\frac{\partial}{\partial\omega}\Sigma_{\rm hom}[\mathbf{k}_2,\omega_0(\mathbf{k}_2)]\right]^{-1}, \tag{49}$$

and ω_0 is given by Eq. (24). To impose the effective-mass approximation we must replace $\Sigma_{\rm hom}(\mathbf{k}\omega)$ by the approximate function given by Eq. (36), which must be obtained by least-squares fitting to $\Sigma_{\rm hom}(\mathbf{k}\omega)$. The least-squares procedure gives

$$\tilde{\Sigma}_{\rm hom}(\mathbf{k}\omega)=\frac{1}{\pi^{3/2}\beta^3}\int d\mathbf{k}_1\,e^{-\mathbf{k}_1^2/\beta^2}\left[\frac{5}{2}-\frac{\mathbf{k}_1^2}{\beta^2}+\left(-\frac{1}{\beta^2}+\frac{2\mathbf{k}_1^2}{3\beta^4}\right)\mathbf{k}^2\right]\Sigma_{\rm hom}(\mathbf{k}_1\omega). \tag{50}$$

The approximate homogeneous-case equations may then be written succinctly in terms of an effective potential which is a function of momentum only,

$$\tilde{V}_{\rm hom}(\mathbf{k})=\tilde{\Sigma}_{\rm hom}(\mathbf{k},\omega_0(\mathbf{k})), \tag{51}$$

as

$$\tilde{V}_{\rm hom}(\mathbf{k}_1)=\int_{|\mathbf{k}_2|<k_f} d\mathbf{k}_2\,K\left(\mathbf{k}_1,\mathbf{k}_2,\tilde{V}_{\rm hom}(\mathbf{k}_1)+\tilde{V}_{\rm hom}(\mathbf{k}_2)+\frac{\mathbf{k}_1^2+\mathbf{k}_2^2}{2m}-2\mu\right)\tilde{\rho}(\mathbf{k}_2), \tag{52}$$

and

$$\tilde{\rho}(\mathbf{k}_1)=\left\{1-\int_{|\mathbf{k}_2|<k_f} d\mathbf{k}_2\frac{\partial}{\partial\omega}K\left(\mathbf{k}_1,\mathbf{k}_2,\tilde{V}_{\rm hom}(\mathbf{k}_1)+\tilde{V}_{\rm hom}(\mathbf{k}_2)+\frac{\mathbf{k}_1^2+\mathbf{k}_2^2}{2m}-2\mu\right)\tilde{\rho}(\mathbf{k}_2)\right\}^{-1}, \tag{53}$$

where

$$K(\mathbf{k},\mathbf{k}_2,\omega)=\frac{1}{\pi^{3/2}\beta^3}\int d\mathbf{k}_1\,e^{-\mathbf{k}_1^2/\beta^2}\left[\frac{5}{2}-\frac{\mathbf{k}_1^2}{\beta^2}+\left(-\frac{1}{\beta^2}+\frac{2\mathbf{k}_1^2}{3\beta^4}\right)\mathbf{k}^2\right]\left\langle\frac{\mathbf{k}_1-\mathbf{k}_2}{2}\left|T_{\mathbf{k}_1+\mathbf{k}_2}(\omega)\right|\frac{\mathbf{k}_1-\mathbf{k}_2}{2}\right\rangle. \tag{54}$$

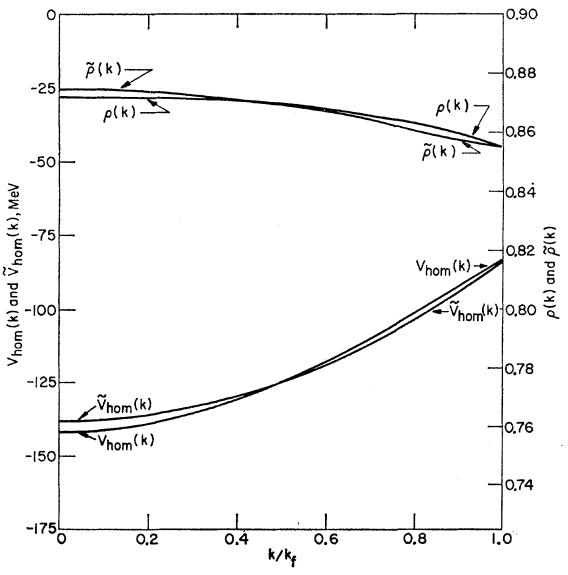

FIG. 2. Effective potential $\tilde{V}_{\rm hom}(k)$ and momentum distribution $\tilde{\rho}(k)$ as functions of k/k_f for the homogeneous-case Puff-Martin approximation using an effective-mass approximation. The corresponding function $V_{\rm hom}(k)$ and $\rho(k)$ without the effective-mass approximation are also shown. Both the effective-mass and exact solutions are evaluated at the local-transport zero point, and both solutions give a cutoff momentum of $k_f=1.6865$ F^{-1}.

Note that it is the approximate $\tilde{\Sigma}(\mathbf{k}\omega)$ rather than $\tilde{V}(\mathbf{k})$ which is quadratic in $\mathbf{k}$.

These homogeneous-case effective-mass equations were solved for the local-transport zero point in the manner described in reference 1. The weighting parameter β (which we had left arbitrary) was adjusted to give the same value of $k_f=1.6865$ F^{-1} in the effective-mass calculation as was obtained in the exact calculation; this led to a value of $\beta=0.8931$ F^{-1}. The results

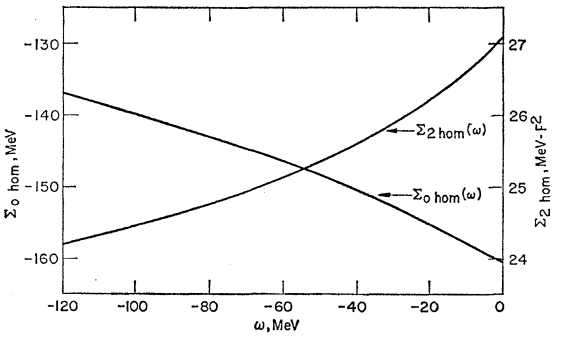

FIG. 3. The coefficients of the effective-mass approximation [Eq. (36)] for the self-energy in the homogeneous case. The constant term $\Sigma_{0\,\rm hom}(\omega)$ and the quadratic term $\Sigma_{2\,\rm hom}(\omega)$ are given as functions of ω.

for $\tilde{V}_{\text{hom}}(\mathbf{k})$ and $\tilde{\rho}(\mathbf{k})$ are shown in Fig. 2, along with the corresponding exact solutions, and the results for $\Sigma_{0\,\text{hom}}(\omega)$ and $\Sigma_{2\,\text{hom}}(\omega)$ are shown in Fig. 3. Table II gives a comparison of various nuclear parameters obtained from the effective-mass and exact solutions.

V. RESULTS

The numerical solution of the equations we have derived for a plane nuclear surface was obtained using an electronic computer. An iterative method was employed in which an initial guess for the self-energy was used to compute wave functions which were in turn used to compute a better self-energy.

A preliminary computation was made to obtain a large table of the integration kernel (47), or more precisely a table of coefficients for performing the integrations in Eq. (46) numerically. Then the iterative computation was performed by alternately solving the wave equation (33) (using a modified Noumerov method) with the normalization specified by Eq. (37), and then integrating the wave functions according to Eq. (46) to obtain a new self-energy. After ten iterations, the results of each iteration were identical to the previous results, except for a slight displacement along the z axis towards the vacuum side. This displacement was about 1/75 F, which is small enough to be attributed to numerical errors in the spatial boundary conditions.

TABLE II. Parameters of homogeneous nuclear matter at the local-transport (L-T) zero point, using the exact and effective-mass Puff-Martin approximation.

	Exact	Eff. mass	
Cutoff momentum k_f	1.6865	1.6865	F^{-1}
Chemical potential μ	−24.028	−24.766	MeV
Density ρ^a	0.06991	0.06982	F^{-3}
Interparticle spacing r_0	0.949	0.949	F
Energy density ϵ^a	−1.1903	−1.2323	MeV-F^{-3}
Energy per particle ϵ/ρ	−17.026	−17.649	MeV
μ pressure $P_\mu{}^a$	−0.4895	−0.4969	MeV-F^{-3}
L-T pressure $P_{\text{L-T}}{}^a$	0.0	0.0	MeV-F^{-3}

[a] These quantities must be multiplied by a degeneracy factor of 4.

The resulting self-energy, after the tenth iteration, is shown in Figs. 4 and 5. Figure 6 gives the corresponding results for the particle and energy densities,

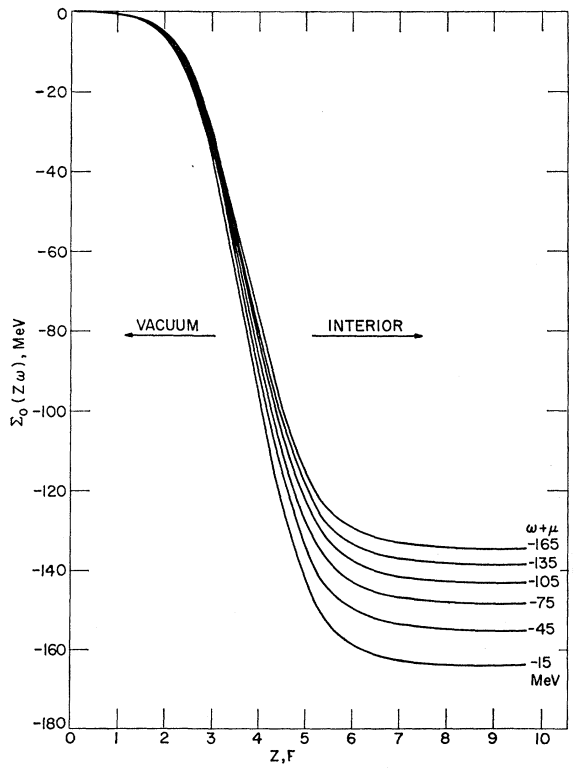

FIG. 4. The momentum-independent term $\Sigma_0(Z\omega)$ of the effective-mass approximation (Eq. 32) for the self-energy across a plane surface. The quantity is given as a function of Z for selected values of $\omega+\mu$, where $\mu=-24.766$ MeV.

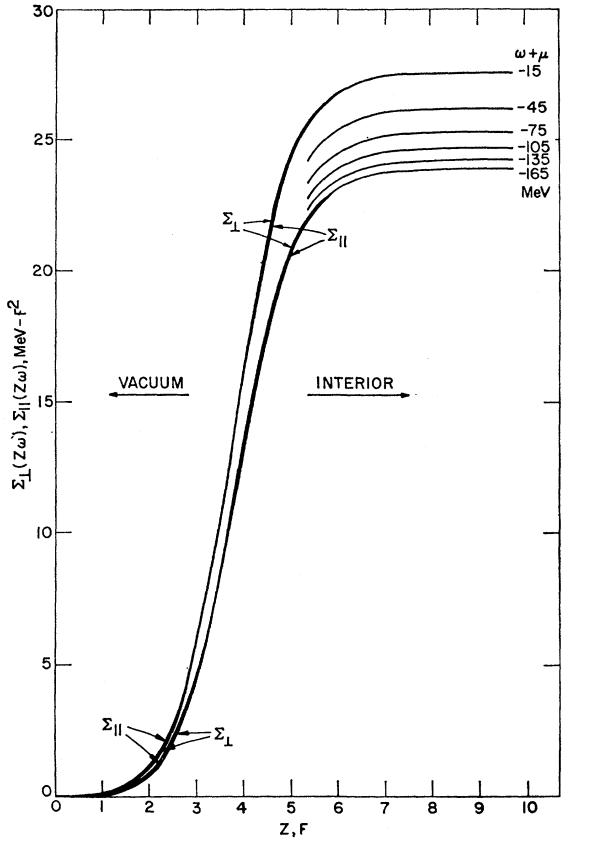

FIG. 5. The quadratic terms $\Sigma_\perp(Z\omega)$ and $\Sigma_{\parallel}(Z\omega)$ of the effective-mass approximation (Eq. 32) for the self-energy across a plane surface. These terms are given as functions of Z for selected values of $\omega+\mu$, where $\mu=-24.766$ MeV. For clarity only the curves for $\omega+\mu=-15$ and -165 MeV are continued into the vacuum region. The two terms $\Sigma_\perp$ and $\Sigma_{\parallel}$, which are coefficients of the momentum components perpendicular and parallel to the Z axis, are equal to within the limited accuracy of the graph, except in the shoulder regions where a small difference is indicated by splitting the curves.

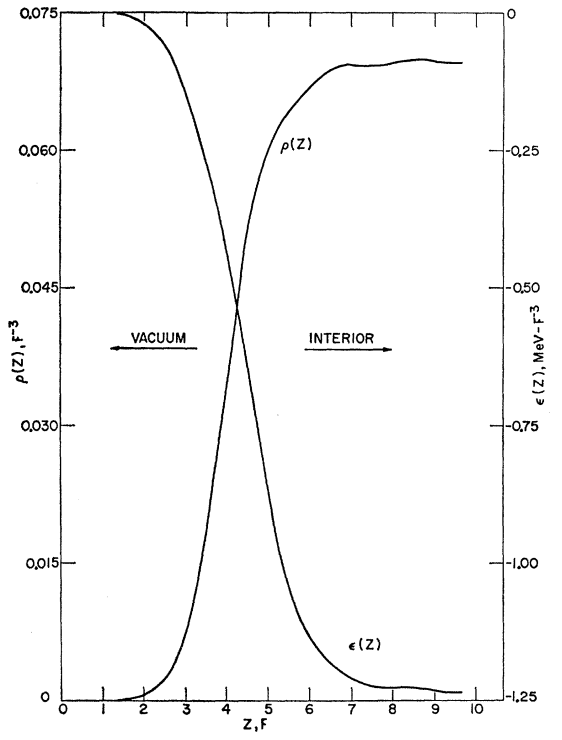

FIG. 6. The particle density $\rho(Z)$ and the energy density $\epsilon(Z)$ across a plane surface, as functions of Z. Both $\rho(Z)$ and $\epsilon(Z)$ must be multiplied by a degeneracy factor of 4.

as calculated from Eqs. (13) and (14) with the substitution of the partial Fourier transform and wave-function expansion of A. Qualitatively, the most significant features of these results are the small difference between $\Sigma_\perp$ and Σ_{II}, which indicates that the self-energy is nearly isotropic, and the general smoothness of the curves, particularly in the region just inside the surface.[5] The most important quantitative result is the surface thickness, i.e., the distance in which the particle density rises from 10 to 90% of its asymptotic value in the interior, which is 2.33 F. This may be compared with a value of 2.5±0.2 F obtained from high-energy electron scattering data.[6]

The results for the particle and energy densities may also be used to compute the surface energy term in the Weizsäcker semiempirical mass formula. Consider a large spherical nucleus; its particle and energy densities, as functions of radial distance, should possess the same shape and height as our calculated $\rho(z)$ and $\epsilon(z)$. Thus, the total number of particles and energy of the nucleus should be

$$N=4\pi\int_0^\infty r^2dr\ 4\rho(r_0-r), \tag{55}$$

and

$$E=4\pi\int_0^\infty r^2dr\ 4\epsilon(r_0-r), \tag{56}$$

where the degeneracy factor of 4 has been inserted, and r_0 is a parameter determining the nuclear size. Then

$$E=\frac{\epsilon(\infty)}{\rho(\infty)}N+16\pi\int_0^\infty r^2dr\ s(r_0-r), \tag{57}$$

where

$$s(z)=\epsilon(z)-\frac{\epsilon(\infty)}{\rho(\infty)}\rho(z) \tag{58}$$

is a function which is nonzero only in a region near the surface. Thus, for a sufficiently large nucleus the integration in Eq. (57) may be extended to negative r, and E may be rewritten as

$$\begin{aligned}E&=\frac{\epsilon(\infty)}{\rho(\infty)}N+16\pi\int_{-\infty}^\infty(\mathbf{r}_0-z)^2dz\ s(z)\\&=\frac{\epsilon(\infty)}{\rho(\infty)}N+16\pi r_0^2\int_{-\infty}^\infty dz\ s(z)+O(r_0).\end{aligned} \tag{59}$$

On the other hand,

$$N=\frac{16\pi}{3}\rho(\infty)r_0^3+O(r_0^2), \tag{60}$$

so that

$$[3N/16\pi\rho(\infty)]^{2/3}=r_0^2+O(r_0) \tag{61}$$

and, thus,

$$E=\frac{\epsilon(\infty)}{\rho(\infty)}N+16\pi\left[\frac{3N}{16\pi\rho(\infty)}\right]^{2/3}\int_{-\infty}^\infty dz\ s(z)+O(r_0). \tag{62}$$

A comparison with the Weizsäcker expansion $E=u_vN+u_sN^{2/3}$ determines the surface energy u_s to be

$$u_s=16\pi\left[\frac{3}{16\pi\rho(\infty)}\right]^{2/3}\int_{-\infty}^\infty dz\left[\epsilon(z)-\frac{\epsilon(\infty)}{\rho(\infty)}\rho(z)\right]. \tag{63}$$

A computation of the surface energy from the results in Fig. 6 gives $u_s=18.79$ MeV. This may be compared

[5] This is in contrast to analogous results from a Hartree-Fock calculation which was performed by the author as a preliminary study for the present work. In this calculation, which used a Gaussian interparticle potential fitted to low-energy scattering data with an admixture of space exchange just sufficient to give saturation, the particle density and self-energy showed a marked oscillatory behavior just inside the surface with an overhang (ratio of maximum value to asymptotic value in the interior) of about 1.10 for the self-energy and 1.07 for the density. These oscillations were apparently a standing-wave phenomenon produced by the sharpness of the surface and enhanced by the extreme exchange nature of the interaction, which reduced the tendency of the integration over the wave functions to smooth out the self-energy. The surface thickness was 2.01 F and the self-energy was again nearly isotropic.

[6] B. Hahn, D. G. Ravenhall, and R. Hofstadter, Phys. Rev. **101**, 1131 (1956).

with a value of 17.804 MeV obtained by Green by fitting nuclear masses.[7] Thus, our calculation leads to a surface thickness and surface energy which are both in reasonable agreement with experimental data.

[7] A. E. S. Green, Phys. Rev. **95**, 1006 (1954).

ACKNOWLEDGMENTS

The author wishes to thank Professor Paul C. Martin, Professor Kurt Gottfried, and Professor Robert D. Puff for their enlightening discussions and helpful criticism.

PHYSICAL REVIEW VOLUME 130, NUMBER 5 1 JUNE 1963

Angular Correlations of Cascade Gamma Rays in the Decay of Lu^{172}

MARGARET M. STAUTBERG,* E. BROOKS SHERA,† AND KARL J. CASPER
Department of Physics, Western Reserve University, Cleveland, Ohio
(Received 7 December 1962)

Angular correlation experiments have been performed on the 1095–78.7, 901–1095, 901–78.7, and 1586–78.7 keV γ-ray cascades in Lu^{172}. The results of the directional correlation and polarization correlation measurements on the 1095–78.7 keV gamma rays establish the spin and parity of the 1174-keV excited state as 3+. The other measurements are consistent with previous assignments for the spins and parities of the 1664- and 2075-keV excited states.

INTRODUCTION

THE decay of Lu^{172} has been studied by Wilson and Pool[1] using γ-γ coincidence techniques to determine the order and energies of the electromagnetic transitions. The spin and parity assignments of the various energy levels were based on the apparent presence of rotational band spectra and on the consistency of the transitions between different bands with the appropriate selection rules. The decay scheme was further expanded by Harmatz *et al.*[2] using conversion electron measurements with a magnetic spectrometer. A decay scheme showing some of the essential features determined by these two studies is presented in Fig. 1.

Since the 1174-keV level appears to be the ground state of a rotational band with $K=3$, a spin of 3 was assigned to this level. The branching ratios and intensities were the basis for a positive parity assignment. In addition the 1664-keV and the 2075-keV level were assigned spins of 3 and 4, respectively.

In this work, angular correlation experiments have been performed in order to provide a definite assignment for the spin and parity of the 1174-keV level and to indicate probable assignments for the 1664- and 2075-keV levels.

EXPERIMENTAL PROCEDURE

Lu^{172} was produced by a 2-h irradiation of an enriched sample of Yb_2O_3 with 12-MeV protons in the Oak Ridge National Laboratory 86-in. cyclotron. Lu^{172} has a half-life of 6.7 days and decays by electron capture to levels in Yb^{172}. The only other activity observed to be present in the source was a small amount of Lu^{171} whose γ rays do not interfere with the measurements carried out in this study. It was found that the Lu activity was readily dissolved in HCl while the Yb_2O_3 was relatively insoluble. Therefore, no additional chemical separation was performed.

The mean lifetime of the 78.7-keV level has been

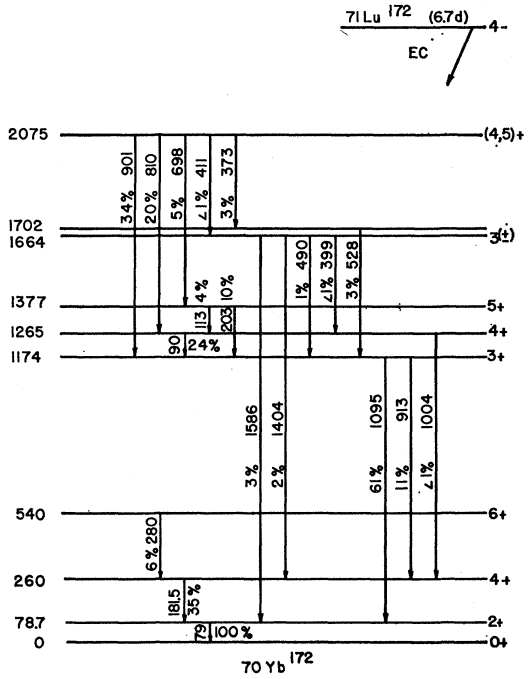

FIG. 1. Decay scheme of Lu^{172}.

* National Science Foundation College Teacher Research Participant. Present address: Department of Physics, University of Massachusetts, Amherst, Massachusetts.

† Present address: Physics Division, Argonne National Laboratory, Argonne, Illinois.

[1] R. G. Wilson and M. L. Pool, Phys. Rev. **118**, 1067 (1960).

[2] B. Harmatz, T. H. Handley, and J. W. Mihelich, Phys. Rev. **123**, 1758 (1961).